


RESEARCH ARTICLE OPEN ACCESS

Mature and Juvenile Neuromuscular Plasticity in Response to Unloading

Michael R. Deschenes^{1,2}  | Max Rackley¹ | Sophie Fernandez¹ | Megan Heidebrecht¹

¹Department of Kinesiology & Health Sciences, College of William & Mary, Williamsburg, Virginia, USA | ²Program in Neuroscience, College of William & Mary, Williamsburg, Virginia, USA

Correspondence: Michael R. Deschenes (mrdesc@wm.edu)

Received: 24 July 2024 | **Revised:** 5 December 2024 | **Accepted:** 4 April 2025

Funding: The work was supported by the Virginia Space Grant Consortium to Max Rackley and The Foundation for Aging Studies and Exercise Science Research to Michael R. Deschenes.

Keywords: adolescence | aging | atrophy | disuse | synapse

ABSTRACT

The neuromuscular junction (NMJ) is the synapse that enables the requisite electrical communication between the motor nervous system and the myofibers that respond to such electrical stimulation with movement and force development. Changes in an NMJ's normal activity pattern have been demonstrated to remodel both the synapse and the myofibers that comprise the NMJ. Significant amounts of research have been devoted to the study of aging on the neuromuscular system. Far less, however, has been focused on revealing the effects of reduced activity on the NMJ and myofibers comprising juvenile neuromuscular systems. In the present investigation, the consequences of decreased activity imposed by muscle unloading (UL) via hindlimb suspension for 2 weeks (a period known to induce muscle remodeling) were examined in both young adult, that is, mature (8 mo), and juvenile (3 mo) neuromuscular systems. In total, 4 treatment groups comprised of 10 animals (Juvenile-Control, Juvenile-Unloaded, Mature-Control, and Mature-Unloaded) were studied. Immunofluorescent procedures, coupled with confocal microscopy, were used to quantify remodeling of both the pre- and postsynaptic features of NMJs, as well as assessing the myofiber profiles of the soleus muscles housing the NMJs of interest. Results of ANOVA procedures revealed that there were significant ($p < 0.05$) main effects for both treatment, whereby UL consistently led to expanded size of the NMJ, and Age where expanded NMJ dimensions were consistently linked with mature compared to juvenile neuromuscular systems. Moreover, only sporadically was interaction between the main effects of Age and Treatment noted. Importantly, one variable that remained impressively resistant to the effects of both Age and Treatment was the critical parameter of pre- to postsynaptic coupling suggesting stability in effective communication at the NMJ throughout the lifespan and despite changes in activity patterns. The data presented here suggest that further inquiry must be performed regarding disuse-related plasticity of the neuromuscular system in adolescent individuals as those individuals regularly suffer injuries resulting in periods of muscle UL.

1 | Introduction

Due in large part to repeated cycles of use and recovery, virtually every physiological system in the human body exhibits considerable plasticity. Such plasticity, or remodeling, has been

documented in the cardiovascular (Poto et al. 2024; Strobel et al. 2024), skeletal (Kubat et al. 2023; LaGuardia et al. 2023), nervous (Filogamo and Cracco 1995; Farrell et al. 2014), respiratory (Mantilla and Sieck 2003; Greene and Riha 2024), digestive (Li et al. 2023; Du et al. 2024; Shin et al. 2024), and renal

This is an open access article under the terms of the [Creative Commons Attribution-NonCommercial](https://creativecommons.org/licenses/by-nc/4.0/) License, which permits use, distribution and reproduction in any medium, provided the original work is properly cited and is not used for commercial purposes.

© 2025 The Author(s). *Developmental Neurobiology* published by Wiley Periodicals LLC.

(Cambien et al. 2024; Georgiyeva et al. 2023; Saritas 2023) systems. Particularly noteworthy is the volume of literature reporting that the neuromuscular system possesses considerable plasticity affecting both myofibers and the motor neurons innervating those fibers along with the neuromuscular junctions (NMJs) which form the synapses joining motor neurons with the myofibers they stimulate to contract and develop force (Sousa-Soares et al. 2023; Deschenes et al. 2022). In fact, there is an abundance of evidence showing that the NMJ is a particularly malleable synapse that responds not only to changes in activity levels (Deschenes et al. 1993; Iyer et al. 2021), but also naturally throughout the lifespan (Kreko-Pierce and Eaton 2018; Valdez et al. 2010; Yamaguchi et al. 2024). Accordingly, it has been shown that both during the developmental stage of adolescence and end-of-life aging, that is, senescence, the NMJ displays a marked capacity for remodeling both physiologically (Yamaguchi et al. 2024) and morphologically (Yamaguchi et al. 2024; Deschenes et al. 2021). Moreover, these two factors (age and physical activity) interact causing amplification of the plasticity typically detected within the neuromuscular system (Deschenes et al. 2021).

Recently, it was reported that with the changes in activity, that is, disuse, resulting from muscle unloading (UL), declines in neuromuscular function, including strength, power, and endurance were substantially more pronounced among aged animals than among young adult ones (Deschenes et al. 2021; Deschenes and Leathrum 2016). This elicited the follow-up question of whether muscle UL would induce greater morphological remodeling of the neuromuscular system among juvenile compared to young adult (mature) animals. It was hypothesized that as the neuromuscular system is in a state of exaggerated plasticity among juvenile animals, muscle UL at this age would result in more pronounced remodeling than among mature ones which tend to show greater stability of morphological features within the neuromuscular system (Deschenes and Leathrum 2016; Dobrowolny et al. 2021).

2 | Experimental Procedures

2.1 | Subjects and Treatment

Twenty young adult (8 months) and 20 juvenile (3 months) male Wistar rats were purchased from Charles River Laboratories (Wilmington, MA, United States). At these ages, rats would be the approximate equivalent of 24 and 9 years of age in humans (Sengupta 2013). For the present project, these age categories were referred to as Mature and Juvenile, respectively. Importantly, at 3 months of age, rats are undergoing a period of rapid accumulation of muscle mass and thus are considered to be an anabolic stage of the normal lifespan (Turturro et al. 1999). Within each age category, half of the animals were randomly assigned to either muscle UL or control (CTL) conditions for the 2-week intervention period, resulting in a total of four treatment groups, each consisting of 9 or 10 individual animals (Mature-UL, Mature-CTL, Juvenile-UL, and Juvenile-CTL). In all cases, muscle UL was imparted with the hindlimb suspension model first described by Morey et al. (1979). In this model, hindlimb muscles are unloaded by preventing the animal's weight-bearing and locomotor activities by elevating its back feet in order to eliminate their contact with the floor. This is achieved by securing adhesive

tape lengthwise along two sides of the rat's tail and attaching a clip to the strips of tape which is then secured to a swivel device with a hook suspended above the animal. This enables the rat to move about in a full 360° arc using its forelimbs. Hindlimb-suspended animals remained in this condition 24 h/day for 14 consecutive days. This time of UL was selected as it has previously been shown to bring about significant muscle morphological remodeling of both NMJs and the myofibers on which they reside (Deschenes et al. 2021, 2022; Deschenes and Leathrum 2016). All unloaded animals were provided with standard rat chow pellets ground to smaller fragments making food easier to handle and thus promoting eating to avoid excessive weight loss during the intervention period. All animals were provided with food and water ad libitum during the experimental period. Environmental conditions included an ambient air temperature of 21°C–22°C and a relative air humidity of ~50%.

Animals selected to CTL conditions were kept individually in plastic tubs lined with wood shavings and provided with water and food ad libitum. These CTL animals were encouraged to move about in their tubs thus enabling normal weight-bearing and locomotor activities. All animal care procedures employed in the current study were approved by the institution's animal care and use committee which operates in full compliance with the National Institutes of Health Guide for the Care and Use of Laboratory Animals as revised in 2011.

2.2 | Cytofluorescent Staining of NMJs

At the conclusion of the intervention period, animals were euthanized via decapitation, following anesthesia resulting from a ketamine-xylazine cocktail injection into the abdominal cavity. Hindlimb muscles, including the soleus, were then surgically removed, quickly cleared of fat and connective tissue, frozen at resting length in isopentane cooled with dry ice, and stored at –80° until analysis. To stain NMJs, 50 µm thick longitudinal sections of the middle one-third of muscles' length were collected with a cryostat (Cryocut 1800; Reichert-Jung, NuBloch, Germany) maintained at –20°C. To prevent contraction of muscle sections, microscope slides were pretreated in a 3% EDTA solution as previously described (Pearson and Sabarra 1974). Staining occurred as follows: sections were first washed 4 × 15 min in phosphate buffered saline (PBS) containing 1% bovine serum albumin (BSA). Sections were then incubated overnight at 4°C in supernatant of the primary antibody RT97 (Developmental Studies Hybridoma Bank, Cat# RT97, RRID:AB_528399), diluted 1:20 in PBS with 1% BSA. The RT97 antibody is sensitive to nonmyelinated segments of presynaptic nerve terminals (Anderton et al. 1982). The following day, sections were washed 4 × 15 min in PBS with 1% BSA before being incubated for 2 h at room temperature in Alexa Fluor 488 conjugated secondary immunoglobulin (Molecular Probes, Eugene, OR, Cat# A11001; RRID:AB_2534069) diluted 1:200 in PBS with 1% BSA. Subsequently, sections were washed 4 × 15 min in PBS with 1% BSA before once again being incubated in a humidified chamber overnight at 4°C in a solution containing rhodamine-conjugated α -bungarotoxin (BTX; Molecular Probes, Eugene, OR, Cat# T1175) diluted 1:600 in PBS with 1% BSA, along with the SV-2 antibody (Developmental Studies Hybridoma Bank, Cat# AB-2315287, RRID:AB-2315387) diluted 1:25 in PBS with 1% BSA. The toxin BTX recognizes and binds to postsynaptic

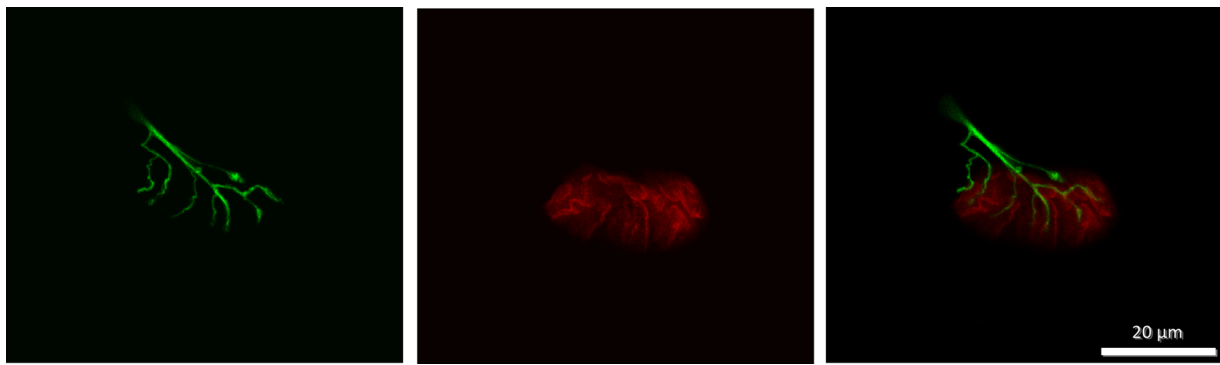


FIGURE 1 | Representative immunofluorescent staining of the NMJ. Presynaptic nerve terminal branches are specifically visualized with the RT-97 primary antibody conjugated with secondary antibody labeled with Alexa Fluor 488 (green), and postsynaptic ACh receptors are identified with bungarotoxin labeled with Alexa Fluor 555 (red). Scale bar = 20 µm.

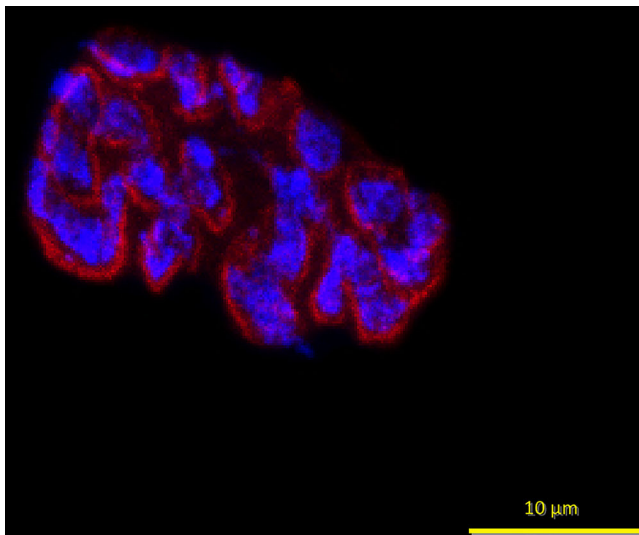


FIGURE 2 | Representative immunofluorescent staining of the NMJ. In this example, presynaptic ACh-containing vesicles are displayed with the SV-2 primary antibody, which is tagged with secondary antibody conjugated to Alexa Fluor 647 (blue), and postsynaptic ACh receptors are identified with Alexa Fluor 555 (red). Scale bar = 10 µm.

acetylcholine (ACh) receptors, and the SV-2 antibody reacts with presynaptic vesicles containing ACh. The following day, sections were again washed 4×15 min in PBS with 1% BSA before incubating them for 2 h in a humidified chamber at room temperature in Alexa Fluor 647 (Molecular Probes, Eugene, OR; RRID:AB_2535813) labeled secondary antibody diluted 1:200 in PBS with 1% BSA to react with and illuminate the SV-2 primary antibody. Sections were then washed again for 4×15 min before being lightly coated with Pro-Long mounting agent (Molecular Probes, Eugene, OR; Cat# P36930) prior to applying cover slips over the muscle sections. Slides were then coded with respect to treatment group to allow for blinded evaluation of NMJ morphology before being stored in the dark at -20°C until analysis was performed. An example of this staining of pre- and postsynaptic components of the NMJ is displayed in Figures 1 and 2.

Presynaptic parameters of NMJs assessed included (1) number of branches identified at the nerve terminal, (2) total length of those branches, (3) average length per branch, and (4) branching complexity which, as described by Tomas et al. (1990), is derived by multiplying the number of branches by the total length of those branches and then dividing that figure by 100. Presynaptic ACh vesicle staining was measured as (1) total perimeter, or the length encompassing the entire vesicular region comprised of both stained vesicular clusters and non-stained regions interspersed within those clusters, (2) stained perimeter, that is, the composite length of tracings around individual clusters of vesicles, (3) total area, which includes stained vesicles along with non-stained regions interspersed among vesicle clusters, (4) stained area, or the cumulative areas occupied by ACh vesicular clusters, and (5) dispersion of vesicles, which was quantified by dividing the vesicular stained area by its total area and then multiplying by 100.

Postsynaptic variables of interest included: (1) total perimeter length, or the length encompassing the entire endplate comprised of stained receptor clusters and non-stained regions interspersed between those clusters, (2) stained perimeter, or the composite length of tracings around individual receptor clusters, (3) total area, that is, stained receptors along with non-stained regions interspersed among receptor clusters, and (4) stained area, or the cumulative areas occupied by ACh receptor clusters. Finally, to quantify the number of ACh-containing vesicles supported by a given length of nerve terminal branch length, the stained area occupied by vesicles was divided by the total length of branching for that NMJ. Lines denoting total and stained tracings of the NMJ are presented in Figure 3.

In this investigation, pre- to postsynaptic coupling was calculated by dividing the NMJ's postsynaptic stained area by its total length of nerve terminal branching as shown in Figure 4, as well as by assessing the percentage of the area of postsynaptic staining of receptors that was overlapped with staining of presynaptic ACh vesicles as previously shown in Figure 5. To optimize consistency, objectivity and accuracy of making manual measurements of NMJ components, the same individual made all these assessments for all samples. Moreover, that individual remained "blinded" to the treatment group of the NMJ he/she was assessing at all times.

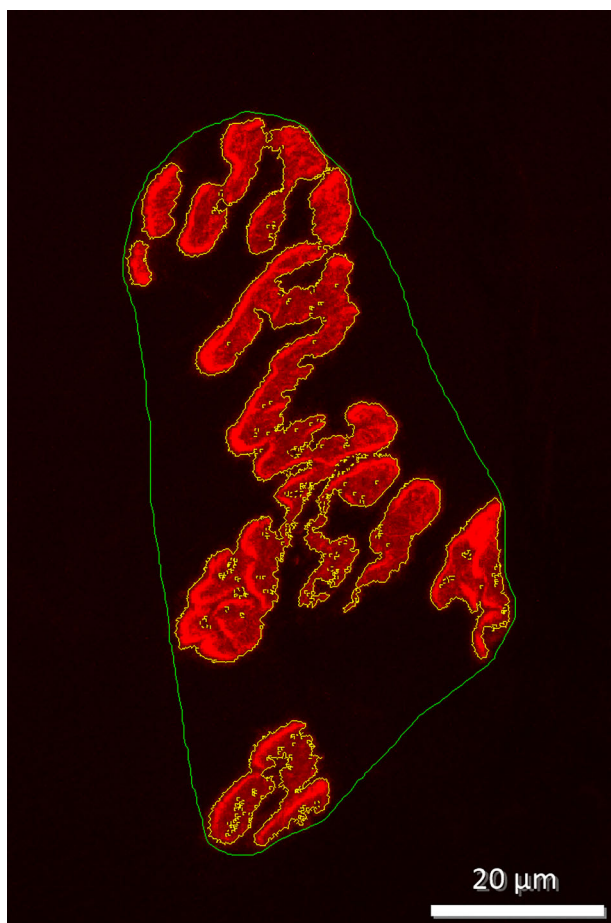


FIGURE 3 | Representative example of tracings for total area and total perimeter length of NMJ are seen with green line encompassing entire structure. Stained area and stained perimeter length are seen with yellow line collectively encompassing entire stained area and entire stained length. Scale bar = 20 μm .

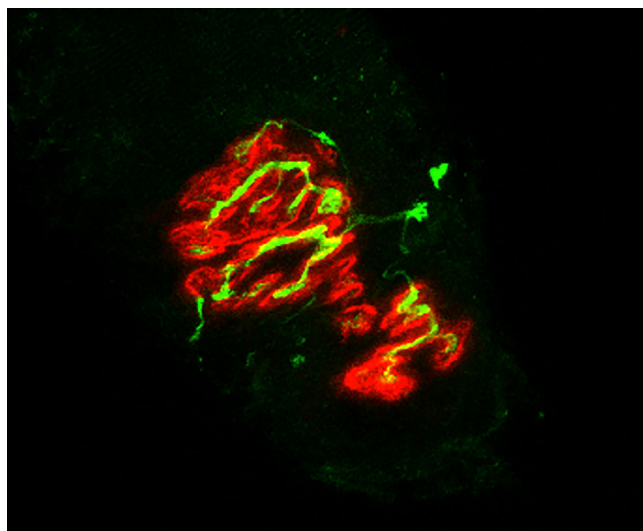


FIGURE 4 | Representative immunofluorescent staining of NMJ pre- to postsynaptic coupling. Presynaptic nerve terminal branches are identified with the RT-97 primary antibody with secondary antibody conjugated with Alexa Fluor 488 (green), and postsynaptic ACh receptors are labeled with bungarotoxin labeled with Alexa Fluor 555 (red). Scale bar = 20 μm .

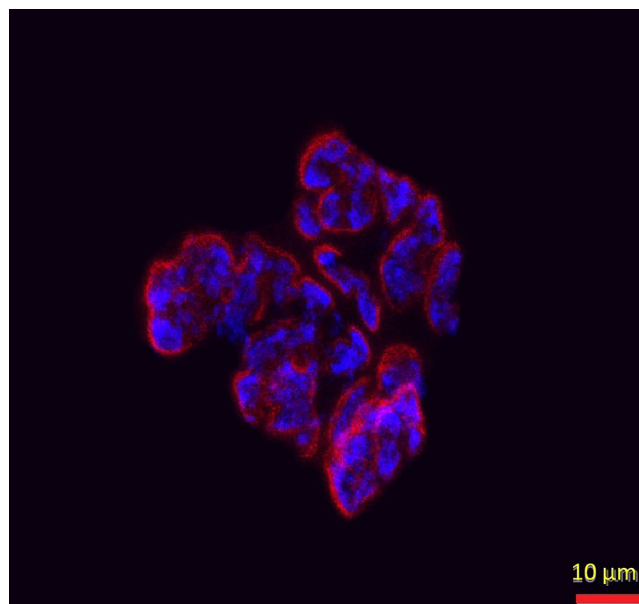


FIGURE 5 | Overlay of presynaptic vesicles with postsynaptic receptors of the NMJ. Coupling is determined as percentage of postsynaptic endplate area also occupied by presynaptic vesicles. Scale bar = 10 μm .

2.3 | Immunofluorescent Staining of Myofibers

To determine myofiber profiles, that is, size and composition, 10 μm thick transverse (cross) sections were first taken from the midbelly of the muscle using a cryostat set at -20°C and then rinsed in PBS with 1% BSA for 5 min. All primary antibodies used to assess myofiber type were obtained from the Developmental Studies Hybridoma Bank at the University of Iowa. These immunogens were initially isolated by Dr. Stefano Schiaffino (Smerdu et al. 1994) and donated to the Hybridoma Bank. The primary antibody BA-D5 (Cat# BA-D5, RRID:AB_2235587) diluted to a concentration of 1:10 in PBS with 1% BSA was used to identify Type I myofibers, whereas SC-71 primary antibody (Cat# SC-71, RRID:AB_2147165) used at a concentration of 1:1 reacted specifically with Type IIA myofibers, and the F3 primary antibody diluted to a concentration of 1:1 was used to identify Type IIB myofibers (Cat# BF-F3, RRID:AB-2266724). Type IIX myofibers were identified by their lack of immunofluorescence (while still being visible via an abundance of background white light). After adding properly diluted primary antibodies, muscle sections were incubated in humidified chambers at 37°C for 1 h. Sections were then rinsed three times for 5 min each in PBS with 1% BSA before being incubated with fluorescently labeled secondary antibodies purchased from Molecular Probes (Eugene, OR, USA) at a concentration of 1:500 in PBS containing 5% goat serum. The secondary antibodies used were conjugated to Alexa Fluor 555 (Cat# A21147, RRID:AB-2535783) to identify Type I myofibers, Alexa Fluor 350 (Cat# A21120, RRID:AB-2535763) to visualize Type IIA myofibers, and Alexa Fluor 488 (Cat# 21042, RRID:AB-2535711) to detect Type IIB myofibers (Figure 6). Following incubation for 30 min at 37°C in humidified chambers, sections were rinsed three times, for 5 min each, in PBS with 1% BSA and then were rinsed for 3 min in deionized water. Excess water was gently removed before Pro-Long Gold (Molecular Probes, Eugene, OR, Cat# P36930) was applied to muscle sections

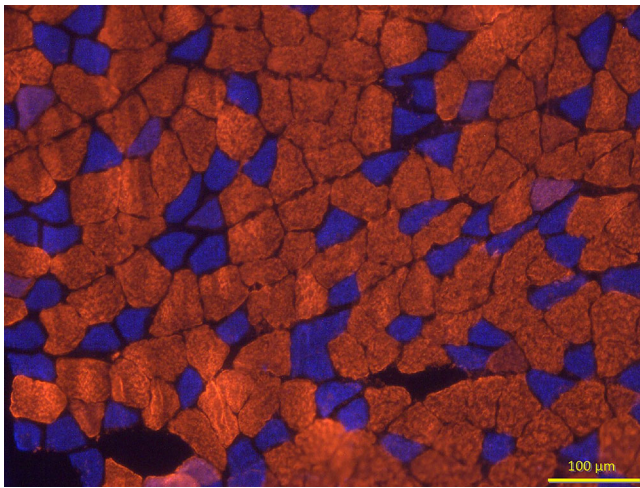


FIGURE 6 | Representative immunofluorescent staining of myofibers. Type I fibers are visualized with Alexa Fluor 555 (red), and Type IIA fibers are stained with Alexa Fluor 350 (blue) secondary antibodies. Type IIB fibers are not expressed in the soleus muscle of the mature rat, and only very few Type IIX fibers were present (remaining unstained). Scale bar = 100 μ m.

that were adhered to microscope slides before applying cover slips on muscle sections and storing slides at -20°C in the dark until analysis was conducted.

2.4 | Microscopy

A confocal scanning system (Olympus FluoView FV 3000) featuring three lasers and an Olympus BX60 fluorescent microscope (Olympus America, Melville, NY) was used to collect and store images of NMJs. Using a 100 \times oil immersion objective, it was initially established that the entire synapse was within the longitudinal borders of the myofiber, that is, “en face” and that damage to the NMJ structure had not occurred during sectioning and staining of the muscle. A detailed image of the entire NMJ was constructed from a z-series of scans taken at 0.5 μ m thick increments. Digitized, two-dimensional images of NMJs were stored on the system’s hard drive and later quantified with the Image-Pro Plus software (Media Cybernetics, Silver Spring, MD). For each muscle, 10–12 NMJs were quantified, and measurements were averaged to represent NMJ morphology within that muscle.

To carry out the quantification of myofiber profiles, an Olympus BX41 microscope with fluorescence capacity (X-Cite, Excelitas Technologies, Ottawa, Canada) was used along with the Infinity Analyze software (Lumenera Corporation, Ottawa, Canada). A random sample of 125–150 myofibers from each muscle was ascertained to determine average myofiber size (cross-sectional area) and % fiber type composition (% of each fiber type analyzed for that muscle).

2.5 | Statistical Analysis

All results are presented here as means \pm SE. All other variables of interest were assessed with two-way ANOVA with main effects for Age (Mature vs. Juvenile) and Treatment (CTL vs. Unloaded)

as well as interaction between main effects. This occurred for each variable of interest, and when indicated, that is, significant interaction, a Tukey post hoc analysis was performed to identify significant pairwise differences. In all analyses, $p < 0.05$ was used to identify statistical significance. Effect size (ES) of differences between groups was also calculated as the difference between group means divided by the standard deviation of the CTL group. In this assessment, ESs of 0.2 represent small differences, whereas an ES of 0.5 is considered a moderate difference, and an ES of 0.8 or larger is considered a large difference. The statistics program StatView by SAS Institute, Inc., Cary, NC was used for all statistical analyses reported here; all data reported here were normally distributed.

3 | Results

3.1 | Whole Muscle Mass

In the present investigation, the soleus was selected for focused study because as a postural, that is, weight-bearing, and locomotor muscle with a high duty cycle, its normal recruitment pattern is severely disrupted by the hindlimb suspension model of disuse and typically undergoes considerable remodeling as a result. The data presented here show that the 2-week muscle UL intervention period resulted in significant ($p < 0.05$) but similar declines in muscle mass in the Juvenile and Mature soleus muscles (29% vs. 36%, respectively; ES = 0.53) that were not found to be statistically significant.

3.2 | Presynaptic Variables

The first presynaptic parameter of interest to be examined was branch number that was quantified with RT-97 staining. Initial ANOVA results indicated a significant main effect for both Age (Mature > Juvenile, ES = 3.6) and Treatment (Unloaded > CTL, ES = 3.0), as well as significant interaction between the two main effects. As a result, a Tukey post hoc analysis showed that the number of terminal branches was significantly less in the Juvenile, CTL NMJs than in all other treatment groups. In assessing branch number, a significant interactive effect was also discerned, and post hoc analysis found that Juvenile, CTL NMJs had greater total branch length than Mature, CTL, and Mature Unloaded NMJs (ES = 3.9 and 2.2, respectively), and that Juvenile Unloaded synapses had significantly less total branch length than both Mature CTLs and Mature Unloaded animals (ES = 5.0 and 3.3, respectively). The focus then turned to average branch length among the four treatment groups. Results showed that there were no main effects for either Age or Treatment for this variable. In contrast, there was a significant interaction with post hoc analysis revealing that Mature, CTL branches, on average, were significantly longer than the branches of all other groups, and that average branch length of synapses from Juvenile, Unloaded animals was significantly shorter than all three other treatment groups. The final metric of presynaptic branch length was branching complexity which is determined as a function of both branch number and length. The initial calculation of complexity revealed that there were significant main effects for both Age (Mature > Juvenile, ES = 2.5) and Treatment (Unloaded > CTL, ES = 5.7), along with significant

TABLE 1 | Presynaptic characteristics of neuromuscular junctions in different treatment conditions.

	Juvenile, Control	Juvenile, Unloaded	Mature, Control	Mature, Unloaded
Nerve terminal branch number	4.7 ± 0.3 ^{*,**}	5.4 ± 0.5	5.8 ± 0.4	6.3 ± 0.3
Total branch length (μm)	73.4 ± 4.8 [*]	66.0 ± 6.7 [*]	97.1 ± 6.1	86.4 ± 2.9
Average branch length (μm)	15.7 ± 0.6	12.1 ± 0.4 [*]	17.1 ± 0.5 [#]	13.8 ± 0.5 [*]
Branching complexity	3.8 ± 0.4 ^{*,**}	4.1 ± 0.7 ^{*,**}	6.3 ± 0.9	6.3 ± 0.5
Total perimeter length (μm)	82.8 ± 3.3 [*]	72.9 ± 2.1 ^{*,**}	99.3 ± 4.7	86.5 ± 4.2
Stained vesicle perimeter length (μm)	162.8 ± 11.7 [*]	176.7 ± 8.7 [*]	241.3 ± 19.2	199.1 ± 17.1 [*]
Total vesicle area (μm ²)	293.2 ± 20.7 [*]	268.5 ± 16.1 [*]	502.7 ± 44.9 ^{***}	360.9 ± 37.8 [*]
Stained vesicle area (μm ²)	63.9 ± 4.0	78.8 ± 3.2	99.7 ± 9.1 ^{****}	82.9 ± 8.2
Pre- to postsynaptic coupling (%) SV-2/BTX	43.7 ± 2.5	49.8 ± 2.7	33.8 ± 2.6 ^{****}	39.1 ± 2.5 ^{***}

Note: Values are reported as means ± SE. *N* = 10 (Juvenile, Control), 8 (Juvenile, Unloaded), 9 (Mature, Control), and 9 (Mature, Unloaded).

^{*}indicates significant difference (*p* < 0.05) from Mature, Control.

^{**}indicates significant difference (*p* < 0.05) from Mature, Unloaded.

^{***}indicates significant difference (*p* < 0.05) from all other groups.

^{****}indicates significant difference (*p* < 0.05) from Juvenile, Control and Juvenile, Unloaded.

interaction between those variables. Post hoc procedures showed that due to the greater lengths of Mature terminal branches, branch complexity was also greater among those terminals. It is noteworthy, however, that Mature terminal branches were longer than Juvenile ones in each of two treatment conditions examined, that is, CTL and Unloaded. The amplifying effect of UL on branching was not unsurprising as several investigations had previously reported that disuse provoked an increase in number of branches per NMJ and total length of branching at the NMJ (Deschenes and Leathrum 2016; Fahim 1989; Deschenes et al. 2013; Brown and Ironton 1977). It is believed that with the decline of neuromuscular activity, the nerve terminal sprouts new branches in an attempt to reestablish normal neuromuscular communication of the NMJ (Fahim 1989; Deschenes et al. 2013; Brown and Ironton 1977). Data on presynaptic nerve terminal branching are presented in Table 1.

To achieve a more comprehensive assessment of presynaptic plasticity, presynaptic ACh-containing vesicles were examined. Manual, or hand drawn, perimeter length—including both stained vesicles and the unstained regions interspersed between clusters of vesicles—was the first variable quantified and termed “total length.” Statistical analysis demonstrated main effects for both Age (Mature > Juvenile, *ES* = 19.7) and Treatment (Unloaded > CTL, *ES* = 16.9). In response to significant interaction between the two primary variables of interest, post hoc analysis for interaction showed that Mature, CTL NMJs had longer perimeter lengths than the three other treatment groups, and that Juvenile, Unloaded presynaptic perimeter lengths were significantly shorter than the three other treatment groups. Moreover, it was determined that for both Juvenile and Mature synapses, UL evoked significant reductions in perimeter lengths around presynaptic vesicle staining. In addition to measuring hand drawn perimeter lengths encompassing presynaptic vesicle staining, the Image-Pro Plus program used also provided precise measurements, collectively, around individual clusters of presynaptic vesicles. As with hand drawn perimeter lengths, computer generated lengths also displayed significant main effects for both Age (Mature > Juvenile, *ES* = 10.5) and Treatment

(Unloaded > CTL, *ES* = 9.7), as well as interaction between those two main variables. Post hoc analysis showed that perimeter lengths encompassing ACh vesicles were longer among Mature, CTL muscles than muscles from all three other treatment groups.

The next presynaptic variable quantified was total area, that is, stained clusters along with unstained regions interspersed, of ACh vesicle clusters. Again, significant main effects were revealed whereby Mature NMJs > Juvenile NMJs (*ES* = 9.6), and Unloaded synapses > CTL presynaptic ones (*ES* = 7.0). Moreover, significant interaction between Age and Treatment was detected. The post hoc follow-up showed that Mature, CTL presynaptic areas were significantly larger than the three other treatment groups. The final presynaptic variable of interest was area occupied by ACh-containing vesicles, but only of the vesicles themselves, and not the unstained regions between islands (clusters) of stained vesicles. Again, this analysis was performed by the Image-Pro Plus software. In this variable, there were significant main effects for Age (Mature > Juvenile, *ES* = 10.3) and Treatment (Unloaded > CTL, *ES* = 4.9), as well as significant interaction between main effects. Post hoc analysis then indicated that Mature, CTL presynaptic staining exclusively of vesicles and not unstained regions interspersed showed that Juvenile, CTL presynaptic areas were smaller than those of Mature, CTL and Mature, Unloaded NMJs.

3.3 | Postsynaptic Variables

When examining the structural adjustments of postsynaptic endplates to UL in Juvenile and Mature muscles, it was determined that much of what was detected in presynaptic variables was also evident in the postsynaptic endplate regions associated with them. More specifically, there were consistent and significant (*p* < 0.05; *ES* = 3.9–8.8 in Mature CTL vs. Mature, Unloaded; Juvenile, CTL, and Juvenile, Unloaded) main effects for both Age (Mature > Juvenile) and Treatment (Unloaded > CTL). More specifically, in each of the postsynaptic parameters of interest, that is, Bungarotoxin-stained area, Bungarotoxin total

TABLE 2 | Postsynaptic characteristics of neuromuscular junctions in different treatment conditions.

	Juvenile, Control	Juvenile, Unloaded	Mature, Control	Mature, Unloaded
BTX, stained area (μm^2)	155.2 \pm 10.5	161.4 \pm 20.6	244.5 \pm 10.1*	204.2 \pm 12.0**
BTX, total area (μm^2)	349.5 \pm 28.6	324.4 \pm 41.6***	546.2 \pm 31.4*	419.9 \pm 23.5
Total BTX perimeter (μm)	85.3 \pm 3.5	78.3 \pm 5.5	100.5 \pm 2.8**	91.4 \pm 2.0****
Stained perimeter (μm)	204.7 \pm 17.0	179.5 \pm 22.4	264.2 \pm 13.6**	231.9 \pm 11.7****
Pre- to postsynaptic coupling (%) RT97/BTX	47.8 \pm 2.4	43.2 \pm 4.3	39.8 \pm 2.7	42.7 \pm 2.2

Note: Values are reported as means \pm SE. $N = 10$ (Juvenile, Control), 8 (Juvenile, Unloaded), 9 Mature, Control), and 9 (Mature, Unloaded).

*indicates significant ($p < 0.05$) difference from all other groups.

**indicates significant ($p < 0.05$) difference from Juvenile, Control and Juvenile, Unloaded.

***indicates significant ($p < 0.05$) difference from Mature, Control and Mature, Unloaded.

****indicates significant ($p < 0.05$) difference from Juvenile, Unloaded.

area (vesicles and unstained areas between receptor clusters), manually drawn perimeter length around the entire endplate, and the perimeter length of the line automatically drawn around areas of BTX staining, showed significant main effects for Treatment (Unloaded > CTL). Significant interactive effects mainly highlighted that Mature, CTL NMJs were significantly larger than other synapses with commensurate ES (ES = 3.3–7.9 in Mature CTL vs. Mature, Unloaded; Juvenile, CTL, and Juvenile, Unloaded), and this was true of both area and perimeter length measurements encompassing the endplate.

3.4 | Pre- to Postsynaptic Coupling

Finally, in trying to quantify the important variable of pre- to postsynaptic communication at the NMJ, the structural coupling of presynaptic SV-2 (vesicles) staining with postsynaptic BTX (receptors) staining was assessed. The results failed to identify significant main effects for Age or Treatment, although significant interaction was noted. Post hoc analysis showed that Mature, CTL synapses had greater pre- to postsynaptic coupling than Juvenile, CTL synapses and that Juvenile, Unloaded coupling exceeded that of Mature, Unloaded muscles. Coupled staining of RT-97 (branching) and postsynaptic BTX also failed to show significant main or interactive effects (ES = 1.0, 2.9, and 1.3 in Mature CTL vs. Mature, Unloaded; Juvenile, CTL, and Juvenile, Unloaded). Data presenting postsynaptic and pre- to postsynaptic coupling can be found in Table 2.

3.5 | Myofiber Profiles

In addition to NMJs, myofibers play a cardinal role in the neuromuscular system as they demonstrate both excitability (response to neural impulses) and contractility (capacity to develop force). In determining myofiber profiles, immunofluorescent procedures were used to distinguish among different fiber types as determined by expression of subtypes of the myosin heavy chain protein. Using this criterion, fibers are classified as Type I, Type IIA, Type IIX, or Type IIB; it should be noted, however, that Type IIB fibers are not expressed in mature soleus muscles of rats (Delp and Duan 1996). In quantifying myofiber type profiles, it was first determined what the contribution of each fiber type is to the muscle in question and then what

the average myofiber size (cross-sectional area) is for different fiber types under different conditions. Initially, fiber types were pooled/collapsed together to examine what the average fiber size was from muscles of different ages and treatment conditions. Statistical results from this analysis revealed significant main effects whereby Mature and CTL animals featured fibers that were significantly larger than those from the Juvenile and Unloaded groups. When examined by individual fiber type, the predominant Type I fibers of the Mature, CTL soleus muscles were established to be significantly ($p < 0.05$) larger (ES = 4.2, 2.0, and 2.2, respectively, in Mature CTL vs. Mature, Unloaded; Juvenile, CTL, and Juvenile, Unloaded) than Type I fibers from each of the other three treatment groups. In contrast, the fibers of the Juvenile, Unloaded group were significantly smaller than those from each of the other three treatment groups. It was also found that UL resulted in significant and similar fiber atrophy in Mature (34%) and Juvenile (24%) muscles. This was roughly the same age-related difference observed for whole muscle mass (36% and 29%, respectively, in Mature and Juvenile soleus muscles), thus confirming the predominance of Type I fibers in the soleus muscle, that is, 36% and 29%, respectively, in Mature and Juvenile muscles. When examining the effects of disuse on Type I fibers exclusively, the results faithfully reflected what was found when fiber types were pooled together. Specifically, Mature, CTL Type I fibers were significantly larger in cross-sectional area than all other treatment groups, and again Type I fibers of Juvenile, Unloaded muscles were significantly smaller than those from the three other treatment groups. The size of Type IIA fibers, the only other meaningful contributor to muscle fiber profile of the soleus, did not significantly differ among the four treatment groups. The second aspect of myofiber profiles examined was relative contribution of the specific fiber type to all fibers of the muscle. When examining this variable, it was noted that in all four treatment groups, Type I fibers were by far the most commonly expressed fiber type ($\geq 95\%$). In effect, neither Age, nor Treatment impacted fiber type composition of the soleus muscles in the animals examined here. Data regarding myofiber profile are presented in Table 3.

4 | Discussion

Muscle UL is experienced by a great many people throughout the world, and its rate of imposition shows no sign of abating

TABLE 3 | Myofiber profiles of soleus muscles from different treatment groups.

Cross-sectional area (μm^2)	Mature, Control	Mature, Unloaded	Juvenile, Control	Juvenile, Unloaded
Fiber types combined	2976.7 \pm 224.9*	1939.8 \pm 193.0	1716.8 \pm 99.2	1302.5 \pm 123.1**
Type I	2718.2 \pm 362.2*	1976.3 \pm 195.9	1911.9 \pm 98.4	1207.8 \pm 96.1
Type IIA	1417.0 \pm 149.6	1201.5 \pm 126.1	1193.2 \pm 109.5	1294.9 \pm 230.0
Fiber type composition (%)				
Type I	96.2 \pm 1.1	97.0 \pm 0.6	95.4 \pm 1.0	94.7 \pm 1.1
Type IIA	3.8 \pm 0.9	3.0 \pm 0.8	4.6 \pm 0.8	5.3 \pm 0.9

Note: Values are means \pm SE.

*indicates significantly ($p < 0.05$) larger than all other groups.

**indicates significantly smaller than all other groups.

(Liu et al. 2024; Pandit and Agrawal 2006). Muscle UL can be presented in the form of limb immobilization, that is, casting, crutches-assisted ambulation, bed rest, or the more permanent condition of paralysis (Storheim and Zwart 2014). Whatever form muscle UL takes, it results in severely detrimental functional and morphological consequences to the neuromuscular system. Such consequences include muscle atrophy of the affected muscles and their constituent fibers (Storheim and Zwart 2014; Lee Satcher et al. 2024), along with significant declines in muscle strength, power, and endurance (Howard et al. 2020). To a large, but not exclusive extent, the loss of strength is driven by muscle atrophy with functional denervation playing a smaller but meaningful role (Iyer et al. 2021). Increasingly, dysfunction at the NMJ, the pivotal synapse connecting motor neurons with the myofibers they innervate, has been claimed to be the root cause of UL-related denervation in declines of muscle strength (Arnold and Clark 2023; Gonzalez-Freire et al. 2014). Indeed, UL has been associated with impaired transmission of the excitatory neural impulse delivered from the motor neuron to the associated myofibers identified at the specific NMJ of interest (Iyer et al. 2021; Gonzalez-Freire et al. 2014). Because UL has been shown to functionally interfere with neuromuscular transmission to different degrees in young adult and juvenile muscles (Deschenes and Wilson 2003; Alford et al. 1987), it has been suggested that during different stages of the natural lifespan, neuromuscular systems will demonstrate differing degrees of sensitivity to changes in activity. In fact, there is an impressive body of evidence indicating that the greater degree of sensitivity to altered levels of activity results in different decrements of muscle strength among the aged relative to young, adult neuromuscular systems (Deschenes et al. 2015). This age-specific sensitivity to muscle UL presents a real challenge to the rapidly increasing aged fraction of our population (Ismail et al. 2021). Primarily, this is related to the fact that not only are the aged more likely to be confined to muscle UL as a result of injury, that is, accidental falls or postsurgical recovery, but also that when subjected to that intervention, the negative consequences will likely be more pronounced than among young, mature neuromuscular systems (Andonian and Fahim 1989; Naro et al. 2019).

In the data presented here, one of the principal findings was the consistent appearance of a significant main effect for treatment, that is, CTL versus Unloaded. Indeed, in virtually all of the

pre- and postsynaptic variables of interest, save average branch length and pre- to postsynaptic coupling, Unloaded NMJs were of greater size than CTL synapses. In general, it has been shown that decrements in activity are associated with an increase in NMJ dimensions (disuse = larger NMJs), and it is commonly thought that the condition of decreased activity is sensed by both muscle and nervous tissue of the neuromuscular system (Yamaguchi et al. 2024). The lack of neuromuscular stimulation, or decreased communication, is interpreted as a malfunctioning unit that must be replaced or reinforced by increasing presynaptic branch length and thus number of presynaptic vesicles; recall that the average number of vesicles per unit branch length, or packing density, is resistant to remodeling (Deschenes et al. 2023).

Importantly, a recent investigation determined that muscle disuse not only imposes deleterious effects on the NMJ, but also throughout the somatomotor CTL system, including the brain's motor cortex and corticospinal system before reaching the NMJ (Sirago et al. 2023). This, as expected, results in more widespread or pervasive detrimental consequences of neuromuscular disuse. This would also do much to explain why relatively small changes in myofiber and whole muscle size can elicit far greater (~2-fold) disturbances in muscle function, including strength and power. In addition to a significant main effect for Treatment (Unloaded > CTL), the ANOVA performed here also revealed a significant main effect of Age where Mature NMJs showed larger dimensions than those displayed by Juvenile synapses. This was not unexpected as it has been established that the size of NMJs on skeletal muscle faithfully mirrors the size and changes in size of the underlying muscle tissue (Balice-Gordon and Lichtman 1990; Balice-Gordon et al. 1990), and our data show that Mature muscles were larger than Juvenile ones.

In addition to senescence, adolescence represents another stage in the natural life cycle that is associated with heightened sensitivity to muscle UL (Haida et al. 1989; Deschenes et al. 2020). In fact, UL-induced loss of muscle strength and muscle atrophy have been reported to be more pronounced among juvenile neuromuscular systems relative to mature ones and to experience delayed recovery processes once removed from the UL intervention (Deschenes and Wilson 2003; Steffen et al. 1990). In short, it appears that both senescence and adolescence represent stages of the natural lifecycle that are particularly sensitive to

the negative neuromuscular adaptations brought on by muscle UL.

Interestingly, although much research has been conducted to reveal the interaction of aging (senescence) and neuromuscular plasticity, far less has been done to determine how UL influences the neuromuscular systems of young rapidly growing animals. This is particularly true concerning morphological adaptations of adolescent NMJs and myofibers and is of particular concern in view of the fact that a recent study reported on functional responses to UL in juvenile and young adult systems (Deschenes et al. 2021) where loss of strength was more pointed in young adult than mature animals. Importantly, the same muscles from the same animal subjects that were featured in that study of function were used here to investigate structural neuromuscular adaptations to muscle UL in those same two age categories. Accordingly, the findings of the present study are of real value for the significant number of adolescent members of our society as it indicates that there is no greater penalty consequent to UL in adolescents than there is for mature neuromuscular systems, at least in the parameters examined here.

The most obvious finding of the present investigation was the presence of significant and consistent main effects for Age (Mature > Juvenile) and Treatment (Unloaded > CTL) on most of the variables of interest. More specifically, of the 14 variables assessed here for NMJ morphology, 12 of them exhibited significant main effects for Treatment and/or Age. Indeed, the only variables not to show a significant main effect for Age or Treatment were pre- to postsynaptic coupling, as well as average branch length which was not surprising in light of our previous works failing to reveal significant plasticity of those variables in response to the effects of age and activity (Deschenes et al. 2021).

Much like the synapses located on their surfaces, myofibers play a critical role in neuromuscular function. And like the NMJs that stimulate them, myofibers are also sensitive to alterations in activity and age (Deschenes et al. 2020, 2022). In view of this, myofiber profiles of soleus muscles from each of the treatment groups were assessed as part of the current investigation. Without concern for specific myofiber type, that is, collapsed across fiber type, it was discovered that cross-sectional area of Mature, CTL myofibers was significantly larger than that observed in all other treatment groups. At the same time the average myofiber size of Juvenile, Unloaded solei was significantly smaller than it was in the three other treatment groups. Overall, the data presented here indicate that the atrophying effect of UL is equally potent in young, adult muscles as it is in juvenile muscles. Similar to earlier research findings (Gerzen et al. 2024; Inns et al. 2022), the data presented here show that both NMJs and the myofibers they reside on are sensitive to the sudden, drastic reductions in neuromuscular activity that comes with UL. Moreover, although it has been shown that long-term disuse is capable of eliciting changes in fiber type expression (Yamaguchi et al. 2024; Brooks and Myburgh 2014), no such trends were noted with the 2-week period of UL employed here where the vast majority of fibers ($\geq 95\%$) were categorized as Type 1.

An especially intriguing finding of the current study was that despite numerous significant instances of structural remodeling of both pre- and postsynaptic components of the NMJ, pre- to

postsynaptic coupling was not altered by UL in either age group studied. This was true whether the presynaptic variable selected for study regarding coupling was nerve terminal branching (RT-97 antibody) or vesicle (SV-2 antibody) staining features. These results suggest that synaptic transmission was not disturbed by the intervention used here, contrasting with earlier results from these same subjects indicating that muscle UL did disrupt neuromuscular transmission efficacy, a functional measure, at least in aged animals (Deschenes et al. 2021); it is noteworthy that aged muscles were not examined here.

It should be considered, however, that the results presented here come from morphological analysis and that functional adaptation to changes in activity patterns and recovery from that intervention do not always mimic those of structure (Davis et al. 2022; Deschenes et al. 2019). And oddly enough, although UL provoked significant atrophy of the affected muscles and their constituent myofibers, the same treatment led to an expansion of the dimensions of juvenile NMJs. This, importantly, suggests that not all components of a single physiological system, in this case the neuromuscular system, necessarily respond in the same way and to the same degree to the same intervention. Here, myofibers and synapses on those fibers responded in opposite fashions with UL causing atrophy in myofibers, while triggering expansion of the NMJs located on those fibers. This unlikely pattern of adaptation should be borne in mind when developing therapy/rehabilitative protocols in clinical settings. Other noteworthy limitations of the present study are that only male animals participated and that these findings cannot necessarily be extended into expectations for females undergoing muscle UL or for periods of UL in excess of 2 weeks, as used here. These two issues require further investigation using female animals and for differing periods of muscle UL. All told, the findings presented here add to the rapidly expanding understanding of the sensitivity and adaptability of the neuromuscular system to alterations in neuromuscular activity and should be of value in both clinical and practical, daily settings.

Author Contributions

Michael R. Deschenes: conceptualization, data curation, formal analysis, project administration, methodology, supervision, writing of original draft. **Max Rackley:** funding acquisition, investigation, visualization, data curation, resources. **Sophie Fernandez:** investigation, visualization, data curation, resources. **Megan Heidebrecht:** data curation, visualization, investigation, methodology.

Conflicts of Interest

The authors declare no conflicts of interest.

Data Availability Statement

The data presented here are available from the corresponding author upon reasonable request.

References

Alford, E. K., R. R. Roy, J. A. Hodgson, and V. R. Edgerton. 1987. "Electromyography of Rat Soleus, Medial Gastrocnemius, and Tibialis Anterior During Hind Limb Suspension." *Experimental Neurology* 96, no. 3: 635–649.

- Anderton, B. H., D. Breinburg, M. J. Downes, et al. 1982. "Monoclonal Antibodies Show That Neurofibrillary Tangles and Neurofilaments Share Antigenic Determinants." *Nature* 298, no. 5869: 84–86.
- Andonian, M. H., and M. A. Fahim. 1989. "Nerve Terminal Morphology in C57BL/6NNia Mice at Different Ages." *Journal of Gerontology* 44, no. 2: B43–B51.
- Arnold, W. D., and B. C. Clark. 2023. "Neuromuscular Junction Transmission Failure in Aging and Sarcopenia: The Nexus of the Neurological and Muscular Systems." *Ageing Research Reviews* 89: 101966.
- Balice-Gordon, R. J., S. M. Breedlove, S. Bernstein, and J. W. Lichtman. 1990. "Neuromuscular Junctions Shrink and Expand as Muscle Fiber Size Is Manipulated: In Vivo Observations in the Androgen-Sensitive Bulbocavernosus Muscle of Mice." *Journal of Neuroscience Official Journal Society Neuroscience* 10, no. 8: 2660–2671.
- Balice-Gordon, R. J., and J. W. Lichtman. 1990. "In Vivo Visualization of the Growth of Pre- and Postsynaptic Elements of Neuromuscular Junctions in the Mouse." *Journal of Neuroscience Official Journal Society Neuroscience* 10, no. 3: 894–908.
- Brooks, N. E., and K. H. Myburgh. 2014. "Skeletal Muscle Wasting With Disuse Atrophy is Multi-Dimensional: The Response and Interaction of Myonuclei, Satellite Cells and Signaling Pathways." *Frontiers in Physiology* 5: 99.
- Brown, M. C., and R. Ironton. 1977. "Motor Neurone Sprouting Induced by Prolonged Tetrodotoxin Block of Nerve Action Potentials." *Nature* 265, no. 5593: 459–461.
- Cambien, G., A. Dupuis, M. Belmouaz, et al. 2024. "Bisphenol A and Chlorinated Derivatives of Bisphenol A Assessment in End Stage Renal Disease Patients: Impact of Dialysis Therapy." *Ecotoxicology and Environmental Safety* 270: 115880.
- Davis, L. A., M. J. Fogarty, A. Brown, and G. C. Sieck. 2022. "Structure and Function of the Mammalian Neuromuscular Junction." *Comprehensive Physiology* 12, no. 4: 3731–3766.
- Delp, M. D., and C. Duan. 1996. "Composition and Size of Type I, IIA, IID/X, and IIB Fibers and Citrate Synthase Activity of Rat Muscle." *Journal of Applied Physiology (Bethesda Md.: 1985)* 80, no. 1: 261–270.
- Deschenes, M. R., R. Flannery, A. Hawbaker, L. Patek, and M. Mifsud. 2022. "Adaptive Remodeling of the Neuromuscular Junction With Aging." *Cells* 11, no. 7: 1150.
- Deschenes, M. R., T. E. Hurst, A. E. Ramser, and E. G. Sherman. 2013. "Presynaptic to Postsynaptic Relationships of the Neuromuscular Junction Are Held Constant Across Age and Muscle Fiber Type." *Developmental Neurobiology* 73, no. 10: 744–753.
- Deschenes, M. R., and C. M. Leathrum. 2016. "Gender-Specific Neuromuscular Adaptations to Unloading in Isolated Rat Soleus Muscles." *Muscle & Nerve* 54, no. 2: 300–307.
- Deschenes, M. R., C. M. Maresh, J. F. Crivello, L. E. Armstrong, W. J. Kraemer, and J. Covault. 1993. "The Effects of Exercise Training of Different Intensities on Neuromuscular Junction Morphology." *Journal of Neurocytology* 22, no. 8: 603–615.
- Deschenes, M. R., M. K. Mifsud, L. G. Patek, and R. E. Flannery. 2023. "Cellular and Subcellular Characteristics of Neuromuscular Junctions in Muscles With Disparate Duty Cycles and Myofiber Profiles." *Cells* 12, no. 3: 361.
- Deschenes, M. R., L. G. Patek, A. M. Trebelhorn, M. C. High, and R. E. Flannery. 2021. "Juvenile Neuromuscular Systems Show Amplified Disturbance to Muscle Unloading." *Frontiers in Physiology* 12: 754052.
- Deschenes, M. R., E. G. Sherman, M. A. Roby, E. K. Glass, and M. B. Harris. 2015. "Effect of Resistance Training on Neuromuscular Junctions of Young and Aged Muscles Featuring Different Recruitment Patterns." *Journal of Neuroscience Research* 93, no. 3: 504–513.
- Deschenes, M. R., H. L. Tufts, A. L. Noronha, and S. Li. 2019. "Both Aging and Exercise Training Alter the Rate of Recovery of Neuromuscular Performance of Male Soleus Muscles." *Biogerontology* 20, no. 2: 213–223.
- Deschenes, M. R., H. L. Tufts, J. Oh, S. Li, A. L. Noronha, and M. A. Adan. 2020. "Effects of Exercise Training on Neuromuscular Junctions and Their Active Zones in Young and Aged Muscles." *Neurobiology of Aging* 95: 1–8.
- Deschenes, M. R., and M. H. Wilson. 2003. "Age-Related Differences in Synaptic Plasticity Following Muscle Unloading." *Journal of Neurobiology* 57, no. 3: 246–256.
- Dobrowolny, G., A. Barbiera, G. Sica, and B. M. Scicchitano. 2021. "Age-Related Alterations at Neuromuscular Junction: Role of Oxidative Stress and Epigenetic Modifications." *Cells* 10, no. 6: 1307.
- Du, K., J. H. Jun, R. K. Dutta, and A. M. Diehl. 2024. "Plasticity, Heterogeneity, and Multifunctionality of Hepatic Stellate Cells in Liver Pathophysiology." *Hepatology Communications* 8, no. 5: e0411.
- Fahim, M. A. 1989. "Rapid Neuromuscular Remodeling Following Limb Immobilization." *Anatomical Record* 224, no. 1: 102–109.
- Farrell, K. E., S. Keely, B. A. Graham, R. Callister, and R. J. Callister. 2014. "A Systematic Review of the Evidence for Central Nervous System Plasticity in Animal Models of Inflammatory-Mediated Gastrointestinal Pain." *Inflammatory Bowel Diseases* 20, no. 1: 176–195.
- Filogamo, G., and C. Cracco. 1995. "Models of Neuronal Plasticity and Repair in the Enteric Nervous System: A Review." *Italian Journal of Anatomy and Embryology = Archivio italiano di anatomia ed embriologia* 100, no. SI: 185–195.
- Georgiyeva, K., B. G. Nudelman, H. Kumar, S. Krishnaswamy, and J. Cazzaniga. 2023. "Multiple Thrombotic, Infectious, and Cardiopulmonary Complications Following Laparoscopic Converted to Open Colectomy Procedure: A Case Report and Literature Review." *Cureus* 15, no. 11: e49384.
- Gerzen, O., I. Potoskueva, V. Votnova, et al. 2024. "Mechanical Interaction of Myosin and Native Thin Filament in the Disused Rat Soleus Muscle." *Life Sciences and Space Research* 41: 80–85.
- Gonzalez-Freire, M., R. de Cabo, S. A. Studenski, and L. Ferrucci. 2014. "The Neuromuscular Junction: Aging at the Crossroad Between Nerves and Muscle." *Frontiers in Aging Neuroscience* 6: 208.
- Greene, C. M., and R. L. Riha. 2024. "Environment and Lung Health in a Rapidly Changing World." *European Respiratory Review Official Journal of European Respiratory Society* 33, no. 172: 240057.
- Haida, N., W. M. Fowler, R. T. Abresch, et al. 1989. "Effect of Hind-Limb Suspension on Young and Adult Skeletal Muscle. I. Normal Mice." *Experimental Neurology* 103, no. 1: 68–76.
- Howard, E. E., S. M. Pasiakos, M. A. Fussell, and N. R. Rodriguez. 2020. "Skeletal Muscle Disuse Atrophy and the Rehabilitative Role of Protein in Recovery From Musculoskeletal Injury." *Advances in Nutrition (Bethesda Md.)* 11, no. 4: 989–1001.
- Inns, T. B., J. J. Bass, E. J. O. Hardy, et al. 2022. "Motor Unit Dysregulation Following 15 Days of Unilateral Lower Limb Immobilisation." *Journal of Physiology* 600, no. 21: 4753–4769.
- Ismail, Z., W. I. W. Ahmad, S. H. Hamjah, and I. K. Astina. 2021. "The Impact of Population Ageing: A Review." *Iranian Journal of Public Health* 50, no. 12: 2451–2460.
- Iyer, S. R., S. B. Shah, and R. M. Lovering. 2021. "The Neuromuscular Junction: Roles in Aging and Neuromuscular Disease." *International Journal of Molecular Sciences* 22, no. 15: 8058.
- Kreko-Pierce, T., and B. A. Eaton. 2018. "Rejuvenation of the Aged Neuromuscular Junction by Exercise." *Cell Stress* 2, no. 2: 25–33.
- Kubat, G. B., E. Bouhamida, O. Ulger, et al. 2023. "Mitochondrial Dysfunction and Skeletal Muscle Atrophy: Causes, Mechanisms, and Treatment Strategies." *Mitochondrion* 72: 33–58.
- LaGuardia, J. S., K. Shariati, M. Bedar, et al. 2023. "Convergence of Calcium Channel Regulation and Mechanotransduction in Skeletal Regenerative Biomaterial Design." *Advanced Healthcare Materials* 12, no. 27: e2301081.

- Lee Satcher, R., B. Fiedler, A. Ghali, and D. R Dirschl. 2024. "Effect of Spaceflight and Microgravity on the Musculoskeletal System: A Review." *Journal of the American Academy of Orthopaedic Surgeons* 32, no. 12: 535–541.
- Li, X. Y., J. Q. Chen, A. Aisa, Y. W. Ding, D. Zhang, and Y. Yuan. 2023. "Targeting BRCA-Mutant Biliary Tract Cancer: Current Evidence and Future Perspectives." *Journal of Digestive Diseases* 24, no. 2: 85–97.
- Liu, Z., Y. Guo, and C. Zheng. 2024. "Type 2 Diabetes Mellitus Related Sarcopenia: A Type of Muscle Loss Distinct From Sarcopenia and Disuse Muscle Atrophy." *Frontiers in Endocrinology* 15: 1375610.
- Mantilla, C. B., and G. C Sieck. 2003. "Invited Review: Mechanisms Underlying Motor Unit Plasticity in the Respiratory System." *Journal of Applied Physiology (Bethesda Md. 1985)* 94, no. 3: 1230–1241.
- Morey, E. R., E. E. Sabelman, R. T. Turner, and D. J Baylink. 1979. "A New Rat Model Simulating Some Aspects of Space Flight." *Physiologist* 22, no. 6: S23–S24.
- Naro, F., M. Venturelli, L. Monaco, et al. 2019. "Skeletal Muscle Fiber Size and Gene Expression in the Oldest-Old With Differing Degrees of Mobility." *Frontiers in Physiology* 10: 313.
- Pandit, L., and A. Agrawal. 2006. "Neuromuscular Disorders in Critical Illness." *Clinical Neurology and Neurosurgery* 108, no. 7: 621–627.
- Pearson, J., and A. Sabarra. 1974. "A Method for Obtaining Longitudinal Cryostat Sections of Living Muscle Without Contraction Artifacts." *Stain Technology* 49, no. 3: 143–146.
- Poto, R., G. Marone, S. J. Galli, and G. Varricchi. 2024. "Mast Cells: A Novel Therapeutic Avenue for Cardiovascular Diseases?" *Cardiovascular Research* 120, no. 7: 681–698.
- Saritas, T. 2023. "The Use of Tissue Clearing to Study Renal Transport Mechanisms and Kidney Remodelling." *Current Opinion in Nephrology and Hypertension* 32, no. 5: 458–466.
- Sengupta, P. 2013. "The Laboratory Rat: Relating Its Age With Human's." *International Journal of Preventive Medicine* 4, no. 6: 624–630.
- Shin, J. H., G. Tillotson, T. N. MacKenzie, C. A. Warren, H. M. Wexler, and E. J. C Goldstein. 2024. "Bacteroides and Related Species: The Keystone Taxa of the Human Gut Microbiota." *Anaerobe* 85: 102819.
- Sirago, G., M. A. Pellegrino, R. Bottinelli, M. V. Franchi, and M. V Narici. 2023. "Loss of Neuromuscular Junction Integrity and Muscle Atrophy in Skeletal Muscle Disuse." *Ageing Research Reviews* 83: 101810. <https://doi.org/10.1016/j.arr.2022.101810>.
- Smerdu, V., I. Karsch-Mizrachi, M. Campione, L. Leinwand, and S. Schiaffino. 1994. "Type IIx Myosin Heavy Chain Transcripts Are Expressed in Type IIb Fibers of Human Skeletal Muscle." *American Journal of Physiology* 267, no. 6 pt 1: C1723–C1728.
- Sousa-Soares, C., J. B. Noronha-Matos, and P. Correia-de-Sá. 2023. "Purineric Tuning of the Tripartite Neuromuscular Synapse." *Molecular Neurobiology* 60, no. 7: 4084–4104.
- Steffen, J. M., R. D. Fell, T. E. Geoghegan, L. C. Ringel, and X. J Musacchia. 1990. "Age Effects on Rat Hindlimb Muscle Atrophy During Suspension Unloading." *Journal of Applied Physiology (Bethesda Md. 1985)* 68, no. 3: 927–931.
- Storheim, K., and J. A Zwart. 2014. "Musculoskeletal Disorders and the Global Burden of Disease Study." *Annals of the Rheumatic Diseases* 73, no. 6: 949–950.
- Strobel, H. A., S. M. Moss, and J. B Hoying. 2024. "Isolated Fragments of Intact Microvessels: Tissue Vascularization, Modeling, and Therapeutics." *Microcirculation (New York, N.Y.: 1994)* 31, no. 4: e12852.
- Tomas, J., R. Fenoll, E. Mayayo, and M. Santafé. 1990. "Branching Pattern of the Motor Nerve Endings in a Skeletal Muscle of the Adult Rat." *Journal of Anatomy* 168: 123–135.
- Turturro, A., W. W. Witt, S. Lewis, B. S. Hass, R. D. Lipman, and R. W Hart. 1999. "Growth Curves and Survival Characteristics of the Animals Used in the Biomarkers of Aging Program." *Journals of Gerontology. Series A, Biological Sciences and Medical Sciences* 54, no. 11: B492–B501.
- Valdez, G., J. C. Tapia, H. Kang, et al. 2010. "Attenuation of Age-Related Changes in Mouse Neuromuscular Synapses by Caloric Restriction and Exercise." *Proceedings of the National Academy of Sciences of the United States of America* 107, no. 33: 14863–14868.
- Yamaguchi, T., K. Kouzaki, K. Sasaki, and K. Nakazato. 2024. "Alterations in Neuromuscular Junction Morphology With Ageing and Endurance Training Modulate Neuromuscular Transmission and Myofibre Composition." *Journal of Physiology* 603, no. 1: 107–125.